ISSN: 1538-4101 (Print) 1551-4005 (Online) Journal homepage: http://www.tandfonline.com/loi/kccy20

Large oncosomes mediate intercellular transfer of functional microRNA

Matteo Morello, Valentina Minciacchi, Paola de Candia, Julie Yang, Edwin Posadas, Hyung Kim, Duncan Griffiths, Neil Bhowmick, Leland Chung, Paolo Gandellini, Michael Freeman, Francesca Demichelis & Dolores DiVizio

To cite this article: Matteo Morello, Valentina Minciacchi, Paola de Candia, Julie Yang, Edwin Posadas, Hyung Kim, Duncan Griffiths, Neil Bhowmick, Leland Chung, Paolo Gandellini, Michael Freeman, Francesca Demichelis & Dolores DiVizio (2013) Large oncosomes mediate intercellular transfer of functional microRNA, Cell Cycle, 12:22, 3526-3536, DOI: 10.4161/cc.26539

To link to this article: http://dx.doi.org/10.4161/cc.26539

Cell Cycle 12:22, 3526–3536; November 15, 2013; © 2013 Landes Bioscience

Large oncosomes mediate intercellular transfer of functional microRNA

Matteo Morello[1,†], Valentina R Minciacchi[1,†], Paola de Candia[2], Julie Yang[1], Edwin Posadas[3], Hyung Kim[4], Duncan Griffiths[5], Neil Bhowmick[3], Leland WK Chung[3], Paolo Gandellini[6], Michael R Freeman[1,7,8], Francesca Demichelis[9,10], and Dolores Di Vizio[1,7,*]

[1]Cancer Biology Program; Samuel Oschin Comprehensive Cancer Institute; Cedars-Sinai Medical Center; Los Angeles, CA USA; [2]INGM Istituto Nazionale di Genetica Molecolare; Milan, Italy; [3]Urologic Oncology Program; Samuel Oschin Comprehensive Cancer Institute; Cedars Sinai Medical Center; Los Angeles, CA USA;[4]Department of Surgery; Division of Urology; Samuel Oschin Comprehensive Cancer Institute; Cedars Sinai Medical Center; Los Angeles, CA USA; [5]NanoSight Inc.; Worthington, OH; [6]Department of Experimental Oncology and Molecular Medicine; Fondazione IRCCS Istituto Nazionale Tumori; Milan, Italy; [7]The Urological Diseases Research Center; Department of Surgery; Boston Children's Hospital; Boston, MA USA; [8]Department of Biological Chemistry and Molecular Pharmacology; Boston Children's Hospital; Boston, MA USA; [9]Institute for Computational Biomedicine; Weill Cornell Medical College; New York, NY USA; [10]Centre for Integrative Biology; University of Trento; Trento, Italy

[†]These authors contributed equally to this article.

Keywords: amoeboid blebbing, microvesicle, filtration, large oncosome, exosome, extracellular vesicles, miRNA, prostate cancer

Prostate cancer cells release atypically large extracellular vesicles (EVs), termed large oncosomes, which may play a role in the tumor microenvironment by transporting bioactive molecules across tissue spaces and through the blood stream. In this study, we applied a novel method for selective isolation of large oncosomes applicable to human platelet-poor plasma, where the presence of caveolin-1-positive large oncosomes identified patients with metastatic disease. This procedure was also used to validate results of a miRNA array performed on heterogeneous populations of EVs isolated from tumorigenic RWPE-2 prostate cells and from isogenic non-tumorigenic RWPE-1 cells. The results showed that distinct classes of miRNAs are expressed at higher levels in EVs derived from the tumorigenic cells in comparison to their non-tumorigenic counterpart. Large oncosomes enhanced migration of cancer-associated fibroblasts (CAFs), an effect that was increased by miR-1227, a miRNA abundant in large oncosomes produced by RWPE-2 cells. Our findings suggest that large oncosomes in the circulation report metastatic disease in patients with prostate cancer, and that this class of EV harbors functional molecules that may play a role in conditioning the tumor microenvironment.

Introduction

Extracellular vesicles (EVs) are membrane-enclosed particles released by virtually any cell type into the extracellular milieu and detectable in body fluids.[1-3] Their abundance has been linked to both physiological and pathological conditions, including cancer.[1,4] EVs are heterogeneous, and a formalized nomenclature is still under debate. Most of the current methodologies employed to purify microvesicles are based on differential centrifugation with or without filtration and are cumbersome and time consuming, therefore difficult to apply to the clinical practice. They also result in populations of EVs that are contaminated with one or more types of EV. This scenario is complicated by the fact that the size of most EVs studied to date (~100 nm) is below the detection limits of both light and fluorescent microscopy, and their visualization requires electron microscopy. This is a significant technological barrier that has delayed accurate characterization of different EV populations, thereby inhibiting the elucidation of their biological roles and intrinsic clinical value. Among the best-characterized EVs, exosomes are 30–100 nm particles released to the extracellular space upon fusion of intracellular multivesicular bodies with the plasma membrane.[5] Even though exosomes are ubiquitous, their molecular content can reflect pathological conditions, and quantitative and molecular analyses of exosomes in patients with cancer may provide clinically relevant information.[6]

EVs derived by direct abscission from the plasma membrane have also been described.[1,7,8] Shedding of these EVs can occur following activation of signal transduction pathways and therefore may play a role in intercellular communication in cancer and other conditions. We recently demonstrated the existence of a new class of EVs that can be very large (1–10 μm) and result from the shedding of non-apoptotic plasma membrane blebs that characterize fast-migrating "amoeboid" tumor cells. The shedding of these "large oncosomes" can be induced in prostate cancer (PCa) cells by overexpression of oncoproteins such as MyrAkt1, HB-EGF, and caveolin-1 (Cav-1).[8] Large oncosome formation and shedding was also demonstrated as a result of silencing of the

*Correspondence to: Dolores Di Vizio; Email: Dolores.DiVizio@cshs.org
Submitted: 09/06/2013; Accepted: 09/18/2013
http://dx.doi.org/10.4161/cc.26539

cytoskeletal regulator Diaphanous-related formin 3 (DIAPH3) through an ERK-mediated pathway.[9] In a previous study, using a differential centrifugation method that does not separate large oncosomes from smaller EV, we were able to enrich for large oncosomes by immuno-flow cytometry with 1–10 μm specific size beads. Using this approach, large oncosomes were identified in association with invasive cancer in the circulation of mice, and the feature was corroborated in tumor tissue using tissue immunostains that detect similar-sized particles.[1] Akin to exosomes and oncosomes of smaller size, large oncosomes contain many classes of signaling proteins relevant to cancer. Given their substantially larger volume, large oncosome-enriched fractions potentially represent a more expansive reservoir of biomolecules than does the exosome EV fraction. Large oncosomes also contain nucleic acids, including miRNA, suggesting that, similarly to other EVs, they may mediate horizontal transfer of diverse RNA species within and across tissue compartments and to distant sites through the circulation.[10] The relatively recent finding that miRNA are present in circulating exosomes[11] suggests that characterization of the molecular cargo carried by microvesicle-enclosed miRNA will allow tumor activity and tumor properties to be detected and quantified in EV-enriched fractions.

Here we describe a rapid filtration-based approach for direct separation of large EVs from smaller microvesicles. Applying this new method to cell media, we isolated large EVs in a similar size range to large microvesicles purified by medium speed differential centrifugation, which has been shown to pellet negligible amounts of smaller EVs.[1,12] We profiled non-tumorigenic and tumorigenic prostate cell lines and derived EVs using an Affymetrix miRNA array platform, followed by qRT-PCR validation on large EVs selectively isolated using filtration. Our results show that distinct classes of miRNAs are differentially expressed in EVs derived from tumorigenic in comparison to non-tumorigenic cells, and that large oncosome-enclosed miRNA can induce migration of cancer-associated fibroblasts (CAFs). Finally, we demonstrated that the filtration method is applicable to human platelet-poor plasma, in which Caveolin-1-positive large oncosomes identified patients with metastatic prostate cancer.

Results

Selective isolation of large EVs

In order to rapidly purify large oncosomes, we applied a filtration-based approach to the culture medium of GFP-overexpressing U87 glioblastoma cells, a cell line with a high rate of large oncosome formation compared with other tumor cells (**Fig. 1A and B**). After removing intact cells and cell debris from the culture media by low force centrifugation (2800 g), the supernatant underwent filtration in columns (nominal diameter of the pores = 200 nm) for 30 s at 8000 g on a bench centrifuge. Particles larger than 200 nm, retrievable from the top of the filter and positive for GFP, were analyzed and sorted by flow cytometry with specific size beads to selectively quantify particles of 1–10 μm in diameter (**Fig. S1A**).[1] Sorted particles were observed by microscopy, which showed large intact vesicular structures in the correct size range (**Fig. 1C**).

To test the efficacy of the filtration approach, we employed flow cytometry analysis to compare the size distribution of the

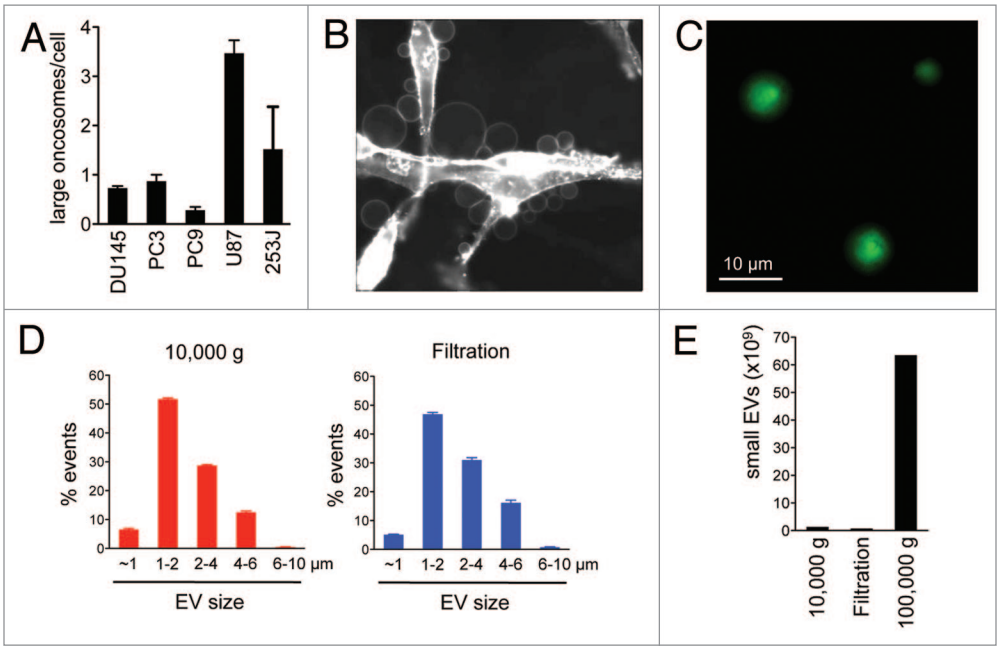

Figure 1. Comparison between different methods of EVs purification. (**A**) Large oncosome formation assay in prostate cancer (DU145, PC3), lung cancer (PC9), glioblastoma (U87), and bladder cancer (253J) cell lines. (**B**) Numerous large oncosomes identifiable by microscopy in U87 glioblastoma cells stained with CTxB-FITC. (**C**) GFP-positive large EVs, collected using filtration, were imaged by fluorescence microscopy. (**D**) Comparative flow cytometry analysis of EVs isolated from the medium of U87 cells, by differential centrifugation (10 000 g) or filtration. Both methods allow detection of large EVs in a similar size range and modal distribution. (**E**) NTA of EVs isolated from the medium of U87 cells, by differential centrifugation (10 000 and 100 000 g) or filtration. The filtration and the 10 000 g centrifugation results in preparations with negligible amounts of small EVs.

EVs purified by filtration or by medium speed (10 000 g) differential centrifugation. The filtration method was conceived with the goal of retaining the target population on the filter and letting smaller particles (<200 nm) flow through. Retrieval of material on the top of the filter gave rise to a population of large EVs (**Fig. 1D**, right panel) similar in size distribution to the ones purified using the centrifugation method (**Fig. 1D**, left panel). As an independent assessment, we quantified smaller EVs (e.g., exosomes) by nanoparticle tracking analysis (NTA) (**Fig. S1B**),[13] a system that allows quantitation of particles smaller than 1 μm. The number of small EVs obtained using both filtration and centrifugation was minimal when compared with the number of small EVs obtained using high-speed centrifugation (100 000 g), often used to identify exosomes (**Fig. 1E**).[14,15] Collectively, these results indicate that the filtration-based method, similarly to 10 000 g centrifugation, can be used for the rapid isolation of EV preps highly enriched in large oncosomes.

miRNA array analysis of EVs

Using a miRNA array, we sought to analyze the miRNA profile in EVs and their cells of origin to investigate whether miRNA representation was similar or different between benign and tumorigenic epithelial cells and EVs they released. In order to reduce cell type-specific variations, we interrogated an isogenic system, the non-tumorigenic, immortalized prostate epithelial cells RWPE-1, and the tumorigenic, KRAS-transformed RWPE-2 cell line.[15] RWPE-2 cells showed a high rate of constitutive plasma membrane budding and large oncosome shedding in comparison to RWPE-1 cells, irrespective of the presence of EGF or fetal bovine serum (FBS) (**Fig. 2A and B**), corroborating previous results showing that large oncosomes are features of malignant cells.[1,8]

We initially applied an Affymetrix miRNA array to EVs purified with high-speed centrifugation (100 000 g), which gives rise to a mixed population of large and small EVs. Technical replicates showed good signal correlation (**Fig. S2**). We observed a strong correlation between expression levels of the intracellular miRNAs of the 2 cell lines (R = 0.944), consistent with their isogenic origin, and also a significant correlation between the miRNAs detected in the EVs from each of the 2 lines (R = 0.895). However, the correlation was lower when we compared intracellular and EV miRNAs in both the non-tumorigenic and tumorigenic lines (R = 0.706 and 0.649, respectively) (**Fig. 2C**). Relative quantitation of the miRNAs suggested differential representation of selected miRNAs in EVs from RWPE-2 (designated EV2) and RWPE-1 (designated EV1) in comparison with donor cells (**Fig. 3**) and also identified cell type-specific signal, suggesting differential miRNA packaging into EVs from the 2 cell types.

qRT-PCR validation and miRNA profiling of large oncosomes

In order to derive information about the contribution of large oncosomes to the miRNA profile of the mixed EV population, we performed qRT-PCR validation experiments on large EVs obtained by filtration (**Fig. 1C and D**). For this purpose, we randomly selected 15 miRNAs that showed at least 1.5-fold change in one of the following comparisons: EV1 vs. RWPE-1 and/or EV2 vs. RWPE-2. The analysis included 4 miRNAs with Affymetrix-based fold change below the threshold. Two miRNAs with Ct values above 36 were considered non-specific and

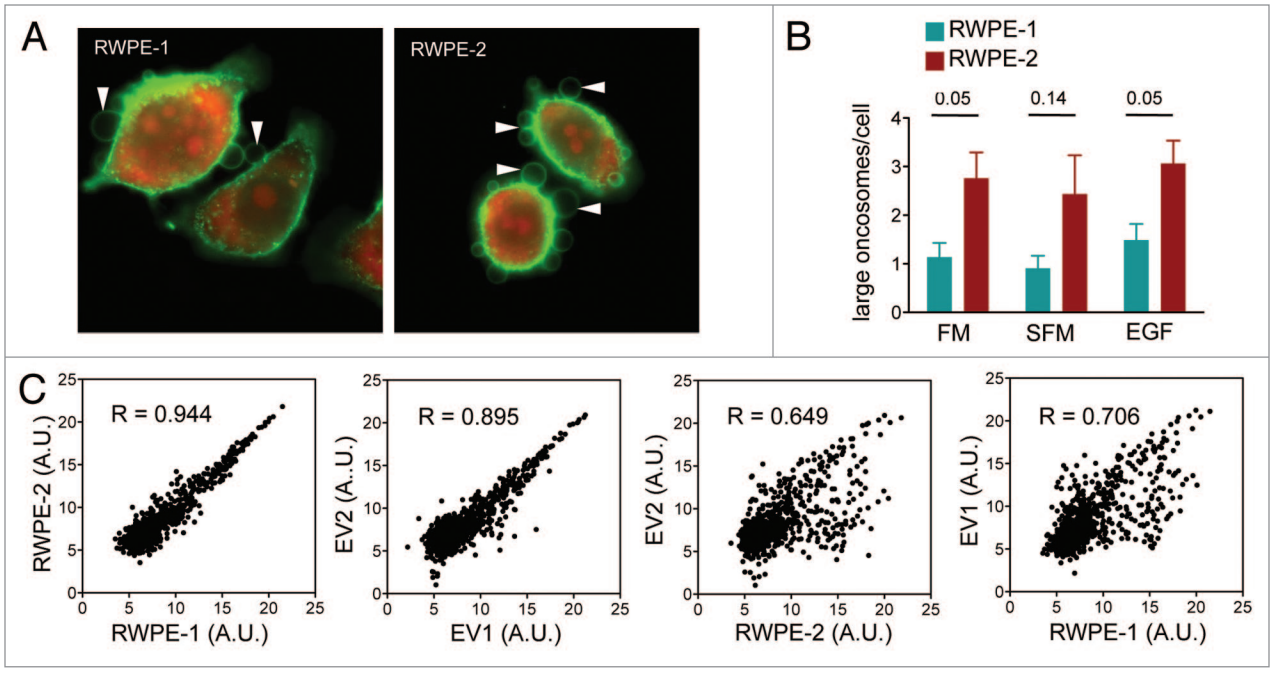

Figure 2. miRNA profiling of prostate cells and derived EVs (Discovery). (**A and B**) Oncosome formation in CTxB-FITC labeled RWPE-1 and RWPE-2 cells, was quantitatively analyzed in presence or absence of full medium (FM), serum-free medium (SFM) and EGF. (**C**) Expression levels of 847 miRNAs in cells and extracellular vesicle. Scatter plots data show the correlation between: RWPE-2 vs. RWPE-1 cells (R = 0.944), EV2 vs. EV1 (R = 0.895), EV1 vs. RWPE-1 cells (R = 0.706) and EV2 vs. RWPE-2 cells (R = 0.649). The difference between EV2 vs. RWPE-2 cells and EV1 vs. RWPE-1 cells indicate an active selection and secretion of miRNA into EV.

were excluded from the downstream analysis. Notably, qRT-PCR analyses of large EVs (**Fig. 3A and B**, bottom row) validated all miRNAs detected as differentially expressed based upon array profiling (top row) of mixed population of EVs. In addition, the majority of miRNAs, whose discovery fold-change values were right below the threshold, demonstrated consistent trends.

The top 5 differentially expressed miRNAs in EV2 vs. RWPE-2 cells, and in EV1 vs. RWPE-1 cells have been described as having both oncogenic and tumor suppressor functions (**Fig. 3C**).[16-20] Importantly, miR-141 and miR-375, both prostate cancer biomarkers,[21,22] were identified in EVs from both cell lines, with slightly higher levels of miR-375 in EV2 than in the donor cell (data not shown). Notably, we identified a subset of miRNAs with at least 1.5-fold expression change in EV2 vs. RWPE-2 cells that did not change significantly in EV1 vs. RWPE-1 cells (**Fig. S3**). Eighteen of these miRNAs were upregulated, while the majority (37 out of 55) were expressed at lower levels in EV2 in comparison with RWPE-2. Interestingly, one of the miRNAs functionally relevant to prostate cancer, miR-205,[23] whose pathological loss seems to favor tumor progression, was identified as an underrepresented miRNA in EV1 and EV2 in comparison to the donor cells.

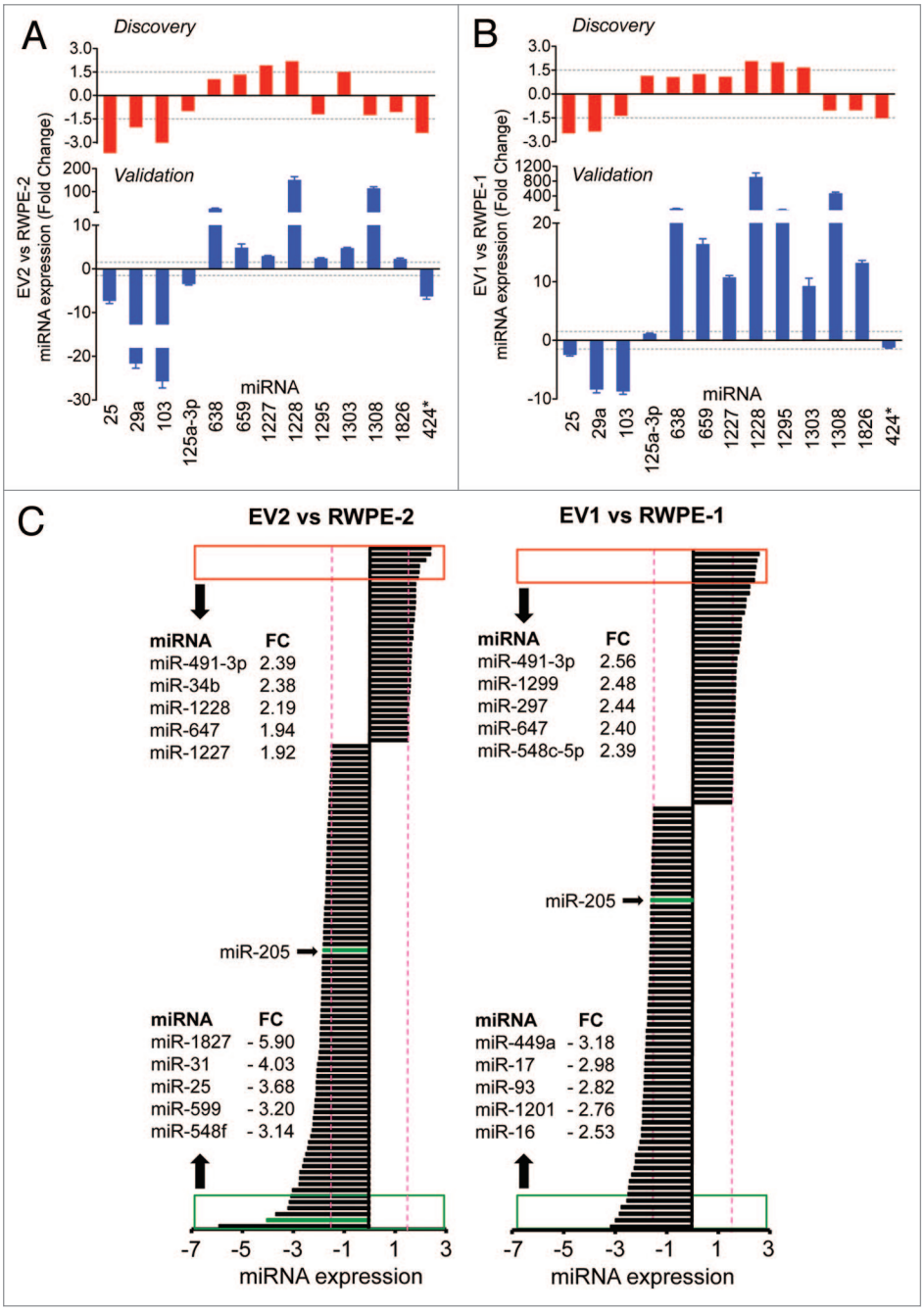

Figure 3. qRT-PCR validation of the discovery experiment using the filtration method, and relative quantitation of miRNAs detected in both EV and donor cells. TaqMan qRT-PCR levels of miRNAs in EV2 vs. RWPE-2 cells (**A**), and EV1 vs. RWPE-1 cells (**B**). (**C**) Relative quantitation of the miRNAs with at least 1.5-fold expression change (red dotted lines) in EV2 vs. RWPE-2 cells (left panel), and in EV1 vs. RWPE-1 cells (right panel). Red and green boxes show the top 5 or bottom 5 expressed miRNAs, respectively.

miRNA-target gene network analysis

In order to identify pathogenic pathways potentially altered by oncosome-associated miRNAs, we performed a network analysis (Ingenuity Pathway Analysis [IPA], http://www.ingenuity.com) of miRNAs with at least 1.5-fold expression difference between EV2 and RWPE-2 donor cells (**Fig. S3**) and with experimentally validated targets (n = 17, target filter [IPA]) (**Fig. 4A**). The network analysis revealed that the top 10 biological functions affected by several of the EV2-enclosed miRNAs include cell proliferation, cell cycle progression, and epithelial neoplasia (**Fig. 4B**), all commonly altered in cancer. Interestingly, most miRNAs with known oncogenic targets were present at low levels in EV2, suggesting that EV from malignant cells are relatively depleted in miRNAs that inhibit the expression of oncogenic proteins.

Targets of most of the miRNAs that were expressed at lower levels in EV2 than in the donor cells include key regulators of cell proliferation, such as the cyclin-dependent kinase CDK6 and the transcription factor E2F1. This group of miRNAs includes miR-182, let-7i, miR-103, miR-107, miR-23a, miR-23b, miR-92a, and miR-149, all with a known role in cancer. Notably, 15 miRNAs, including miR-23b, miR-708, miR130a and miR-149, are involved in tumor cell proliferation, and all of the analyzed miRNAs are involved in epithelial neoplasia. Interestingly, we

found that most EV2-associated miRNAs are also implicated in the regulation of proliferation and differentiation of stroma (**Fig. 4B**). Because these 2 biological functions have been linked to reactive stroma, a hallmark of aggressive cancer,[24] these data suggest that EV-enclosed miRNAs can potentially affect prostate cancer progression by favoring the establishment of a permissive tumor microenvironment. In line with this hypothesis, and relevant to large oncosome function, we show that large EVs isolated both by differential centrifugation and by filtration, induce proliferation of CAFs (**Fig. 4C**).

Large oncosomes induce migration of cancer-associated fibroblasts (CAFs), and the effect is enhanced by miR-1227

Among the miRNAs that exhibited at least 1.5-fold higher levels in EV2 than in EV1 (**Fig. 5A**), we focused our attention on miR-1227, whose overexpression in EV2 vs. RWPE-2 donor cells was validated by qRT-PCR (**Fig. 3A**), and for which functional characterization in cancer cells is lacking. Transient overexpression of a miR-1227 mimic construct in RWPE-2 cells (**Fig. 5B**) resulted in a significant increase of the miRNA levels in the large oncosome fraction (**Fig. 5C**). miR-1227 overexpression in large

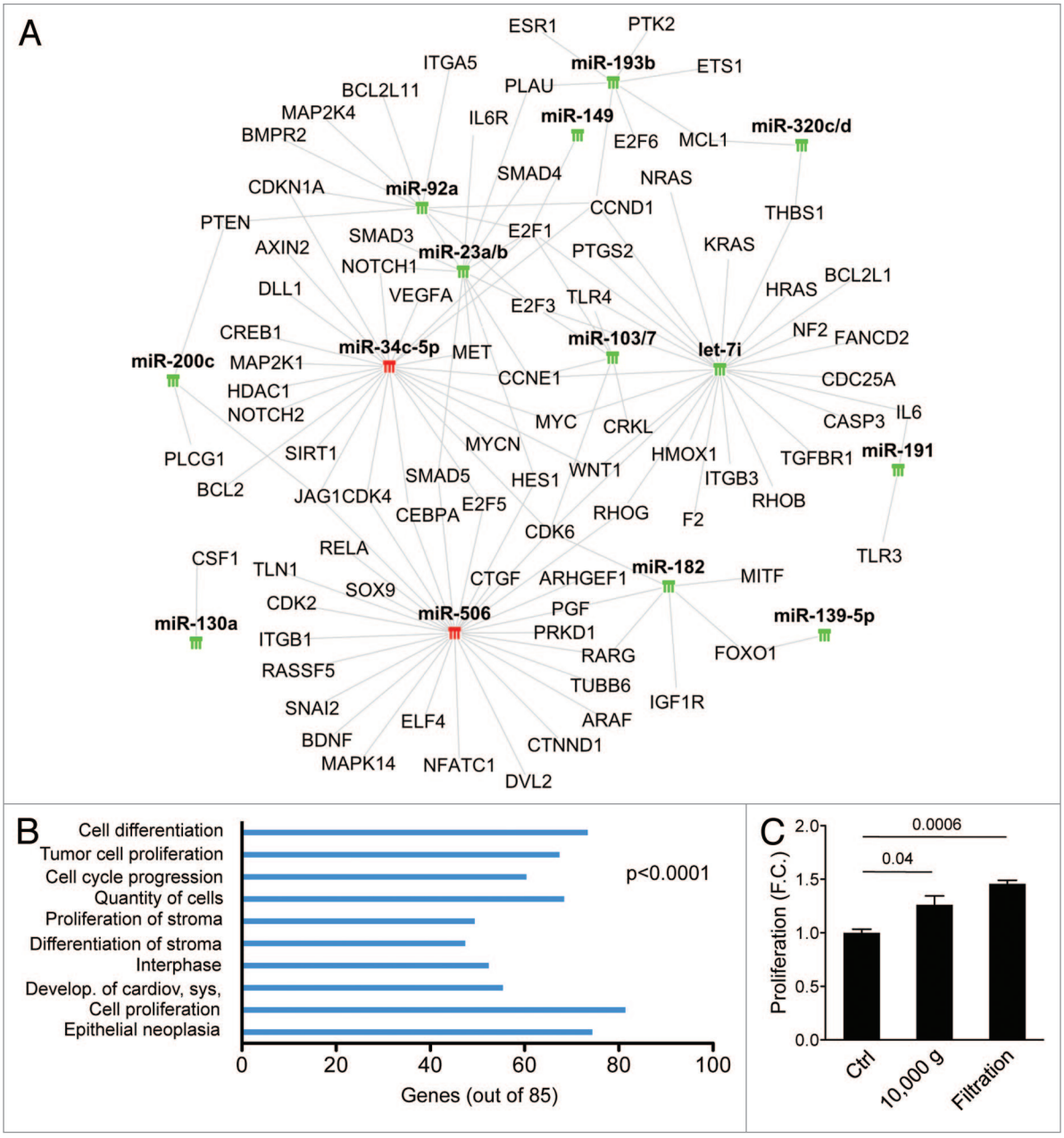

Figure 4. Large oncosomes induce migration of cancer-associated fibroblasts (CAFs), and the effect is enhanced by miR-1227. (**A**) List of miRNAs differentially expressed in EV2 compared with EV1. (**B**) RWPE-2 cells were transfected with miR-1227 mimic, or control vector (miR-NC) and the relative amount of miR-1227 was determined using qRT-PCR at the indicated times. (**C**) qRT-PCR analysis using miR-1227 specific primers was performed on total miRNA isolated from large and small EVs (10 000 and 100 000 g) from RWPE-2 overexpressing miR-1227 mimic. (**D**) Crystal violet assay of CAFs treated for 48 h with large EVs overexpressing miR-1227 mimic or miR-NC showing that overexpression of the miRNA does not affect cell proliferation. (**E**) Migration of CAFs was enhanced by large EVs overexpressing miR-1227.

oncosomes did not influence proliferation of CAFs in comparison to controls, but did induce a significant increase in their migration (**Fig. 5D and E**).

Immuno-capture of large oncosomes using cancer biomarkers

Next we attempted to employ the filtration-based method to isolate green fluorescent protein (GFP)-labeled large oncosomes from the conditioned media of U87 and LNCaP cells stably expressing GFP. Flow cytometry identified abundant GFP-positive EV of 1–10 μm in the media of U87/GFP (**Fig. 6A**), consistent with the observed high production of large oncosomes in that cell type (**Fig. 1A and B**), whereas they were almost undetectable in the media of LNCaP/GFP cells (64.7% and 1.8%, respectively) (**Fig. S4A**), consistent with our previous demonstration of a low rate of large oncosome formation in LNCaP cells.[8] The distribution of the events in relationship to the size is shown in **Figure 6B**, and we confirmed the presence of intact large oncosomes by microscopy (data not shown). Overall, the results indicate that the filtration-based method allows rapid and efficient isolation of large oncosomes from the conditioned media of cancer cells.

We attempted to employ filtration to isolate and quantify large oncosomes from conditioned media of DU145 prostate cancer cells using Cav-1 and ARF6 antibodies against endogenous targets.[8,12] Cav-1 is a validated prostate cancer biomarker found in the circulation of patients with advanced disease,[25] and ARF6 is a GTPase shown to be enriched in large EV and to promote their abscission from cancer cells.[12] Using immuno-flow cytometry with Cav-1 and ARF6 antibodies against preparations obtained from DU145 cell media in combination with the filtration protocol, we detected large EVs positive for both Cav-1 and ARF6 (**Fig. 6C**). Because ARF6 may be a specific marker of large microvesicles, these data suggest that ARF6 and Cav-1 are viable targets for detection and isolation of large oncosomes using immunoaffinity capture in concert with the filtration protocol.

Large oncosomes containing Caveolin-1 can report metastatic disease in patients with prostate cancer

We previously demonstrated that Cav-1-positive large oncosomes, purified using conventional centrifugation-based protocol and analyzed by flow cytometry using sizing beads, were present in the circulation of mice with metastatic prostate cancer.[1] Since the filtration method allowed the rapid isolation of large oncosomes from the cultured media of cancer cell lines, and Cav-1 is a validated prostate cancer biomarker, we next attempted to use this approach to identify large oncosomes in platelet-poor plasma of patients with prostate cancer. Flow cytometry of large EVs purified from 200 μl plasma of 6 patients with low Gleason grade primary tumors and 6 patients with castration-resistant prostate cancer (CRPC) demonstrated a correlation between the number of 1–10 μm Cav-1-positive events and metastatic disease (*P* value = 0.0060) (**Fig. 7**), indicating that large oncosome abundance reflects disease status in patients. These results indicate that the filtration protocol we have described can provide a valid alternative to differential centrifugation methods to isolate and quantify tumor-derived large oncosomes from human blood.

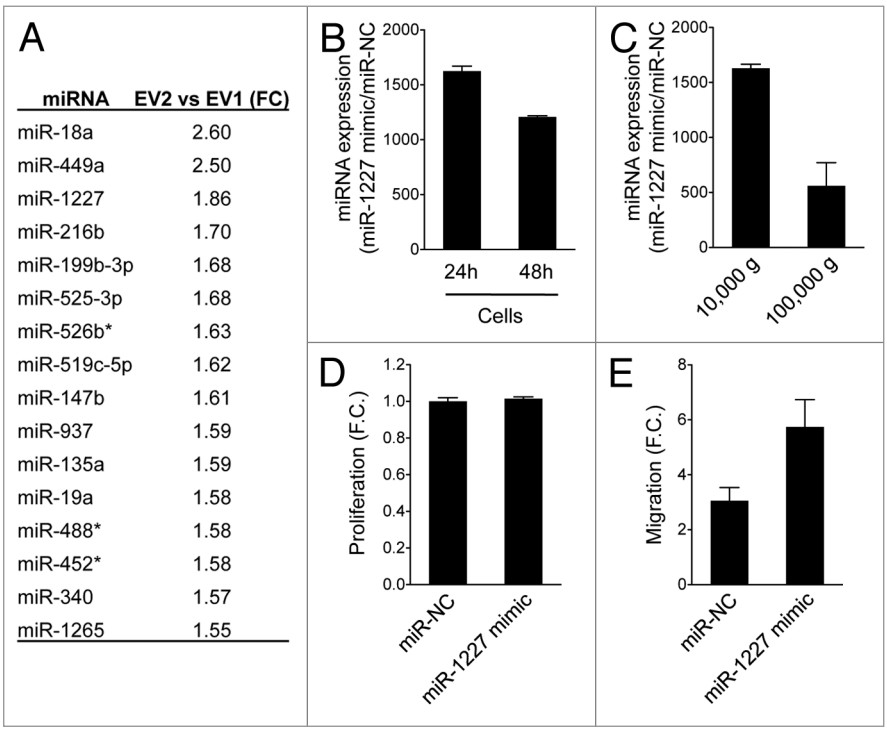

Figure 5. miRNA-target gene network analysis. (**A**) Green and red symbols denote low- and high-expressed miRNAs, respectively. Gray lines indicate inhibitory effect of miRNAs on target genes. (**B**) Target genes of miRNAs expressed at significantly lower or higher levels in EV2 than in RWPE-2 cells, but at non-significantly lower or higher levels in EV1 vs. RWPE-1 cells, were considered for the Ingenuity Pathway Analysis (IPA). Bars indicate the top 10 biological functions in decreasing order of significance. (**C**) Cell proliferation of CAF treated for 48 h with large EVs isolated from RWPE-2 using differential centrifugation (10 000 g) or filtration.

Discussion

This is the first study describing a rapid method, based on filtration, for selective purification of large oncosomes. Using the new method, we demonstrated for the first time that: (1) the number of circulating Cav-1-positive large oncosomes is increased in metastatic in comparison with organ-confined disease in patients with prostate cancer; (2) the method is suitable for molecular profiling of large oncosomes; (3) miRNA analyses indicate that distinct classes of miRNAs are differentially expressed in EVs derived from tumorigenic than from non-tumorigenic cells; (4) miR-1227, which can be preferentially loaded into large oncosomes vs. smaller EV, is a novel modulator of the migration of CAFs.

With the growing realization that EVs play important roles in tumor dissemination and also represent an important source of novel biomarkers,[2,6,26] there is an urgent need to develop standardized, clinically

applicable methods for the isolation and characterization of homogeneous EV subtypes against a background of heterogeneous EV populations. Most methods used currently were developed to characterize nanosized exosomes, and filtration steps purposely exclude larger microvesicles from the preps. Conversely, our filtration-based approach allows selective purification of large oncosomes and should facilitate more extensive characterization of this class of EV. The large oncosome is potentially a significant reporter of cancer activity in the body, given its large volume and content of tumor-derived molecules[1,27-29] (and unpublished observations). One potential caveat of the filtration method is low efficiency, as the total number of particles isolated by filtration is lower in comparison with a medium force speed (10 000 g) used to selectively purify large EVs. However, the observation that we can quantitatively discriminate between metastatic and primary tumor, and the fact that we can analyze the molecular content of large oncosomes, argue in favor of the utility of this method in clinical translation.

The demonstration that the new method is also suitable for analysis of the miRNA cargo of large oncosomes, and that >60% of the miRNAs are expressed at similar levels between donor cells and derived EVs, suggests that some miRNAs are shuttled into the particles because of subcellular location or mass action, indicating that the miRNA content of the particle is representative of the donor cell. Therefore, EVs are a potential source of circulating markers of solid tumor bioactivity or response to therapy. Importantly, prostate cancer miRNA biomarkers miR-141 and miR-375 were identified in EVs. In addition, one of the miRNAs expressed at higher levels in EVs from the tumorigenic cell line, miR-1228, was recently incorporated into a tissue miRNA signature of clinical progression in patients with endometrial carcinoma.[30] Other miRNAs expressed at high levels in EVs from the tumorigenic RWPE-2 subline have not been functionally studied. Interestingly, pathway analysis demonstrated that the top 10 biological functions affected by the 2 miRNAs enriched in EV from the tumorigenic cells are commonly altered in cancer.

Besides the miRNAs expressed at similar levels, our data also show that several miRNAs are differentially expressed in donor cells and EVs, suggesting that the packaging of

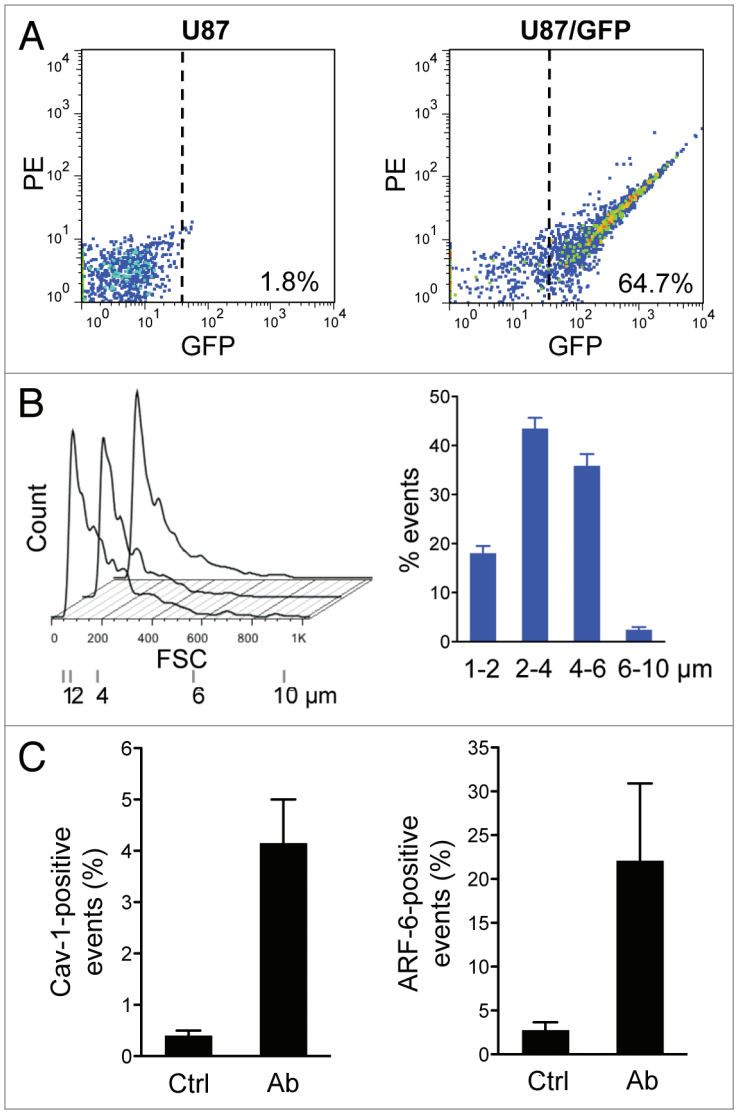

Figure 6. The filtration method allows selective purification of large oncosomes. (**A**) GFP-positive large EVs were purified from the conditioned media of U87/GFP cells by filtration and analyzed by flow cytometry. (**B**) EV size distribution (left) and quantitative analysis (right) as measured by flow cytometry analysis in 3 independent experiments. (**C**) Large EVs, purified from the conditioned media of DU145 cells by filtration, were quantitatively analyzed by immuno-flow cytometry with Cav-1 (left) and ARF6 (right) antibodies.

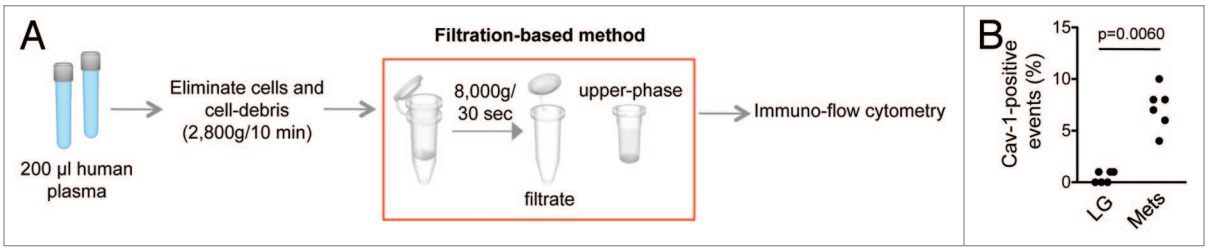

Figure 7. Large oncosomes isolation. (**A**) Workflow showing the filtration-based method for the isolation of large oncosomes. After a low g force centrifugation step to remove intact cells and cell debris, the filtration-based method was employed to purify EVs from human plasma. (**B**) The number of Cav-1-positive large EV in 200 µl of platelet-poor plasma was significantly more abundant in the plasma of patients with metastatic disease (*P* value = 0.0060) than with organ-confined prostate cancer (LG, low-grade Gleason score).

miRNAs into EVs does occur in part by active selection. These data appear consistent with recent findings showing the presence in EVs of transcripts of the membrane vesiculation machinery, as well as nucleic acids encoding essential enzymes for miRNA synthesis.[27] These findings are supportive of the recently proposed hypothesis that miRNA biogenesis occurs within EVs.[31]

While differences in miRNA levels in EVs and donor cells have been reported for other types of cell lines,[32-34] this is the first side-by-side comparison of the miRNA profile of EVs derived from tumorigenic and non-tumorigenic cells. The finding that the top 5 differentially expressed miRNAs in EVs from the tumorigenic subline are distinct from those in the non-tumorigenic subline suggests the possibility that these molecules may alter the tumor microenvironment or distant sites when derived from cancer cells. In line with this hypothesis, our functional studies demonstrated that miR-1227, one of the top 5 differentially expressed miRNAs in EVs from the tumorigenic subline RWPE-2, could elicit biological effects in CAFs (increased cell migration). This result suggests that miR-1227 plays a role in the promotion of migration induced by the large oncosomes, as is the case for other miRNAs carried in different types of EVs.[35] The fact that miR-1227 does not seem to be involved in regulating proliferation of CAFs, while large oncosomes can promote cell proliferation, suggests that large oncosome-mediated effects on proliferation might be dependent on different oncosome cargo. Of interest, the overexpression of a miR-1227 mimic in RWPE-2 cells resulted in a more dramatic increase of the miRNA levels in large oncosomes than in smaller EVs, suggesting an overall larger potential for large oncosomes than for smaller EVs to transfer bioactive molecules between cell compartments.

The finding that a considerable number of miRNAs described as tumor suppressors in several types of tumors, including prostate cancer,[22,36-45] were underrepresented in EVs from the tumorigenic RWPE-2 cell line might be a simple reflection of overall low miRNA expression in prostate cancer in comparison with normal tissue, and of progressively lower miRNA expression with progression to advanced disease.[46] It is interesting that miR-205, which has a known tumor-suppressor function and is lost in advanced disease,[46-48] was not loaded at high levels in EV1 and EV2 in comparison to other miRNAs. This suggests the possibility that tumor suppressor miRNAs may be present at relatively low levels in EV from malignant cells.

Our results suggest that Cav-1-positive large oncosomes can report metastatic disease in patients with prostate cancer, as demonstrated quantitatively by immuno-flow cytometry of the purified vesicles. We recently showed that the number of plasma-derived Cav-1 large oncosomes correlates with disease progression in a mouse model of prostate cancer.[1] In the same study, we showed that large oncosomes identified in prostate cancer tissues in situ could discriminate aggressive disease.[1] However, the findings reported here are the first demonstration of the potential clinical significance of circulating Cav-1-positive large oncosomes in patients with cancer. Because this analysis was performed on 200 μl of plasma, a much smaller amount than what has been reported in virtually all other studies on EV purification from biological fluids, the result suggests that this or a similar approach may have clinical utility. Given their size and the possibility of identifying large oncosomes in tissues by microscopy,[1] the molecular characterization of these EVs might be validated by in situ detection of altered transcripts and other molecules initially identified in the circulation of patients with cancer.

In conclusion, large oncosome characterization can provide clinically valuable information in patients with cancer, and a focus on this large class of EVs may benefit functional and molecular studies.

Materials and Methods

Cell culture

RWPE-1, RWPE-2, LNCaP, and DU145 cells were from the American Type Culture Collection (ATCC). U87 cells were a gift from Dr Michael Klagsbrun, Boston Children's Hospital. The base medium for RWPE-1 and RWPE-2 cell lines was Keratinocyte Serum-Free Medium (K-SFM), supplemented with 0.05 mg/ml bovine pituitary extract (BPE) and 5 ng/ml epidermal growth factor (EGF), 100 U/ml penicillin, and 100 μg/ml streptomycin. For the generation of LNCaP/GFP and U87/GFP cells, parental LNCaP and U87 cells were plated at 70–80% confluence and transfected using Lipofectamine™ 2000 (Life Technologies) with the plasmid pEGFP-C3. Stable populations were isolated following selection with Geneticin G418 0.5 mg/ml (LNCaP/GFP) and 0.4 mg/ml (U87/GFP). LNCaP, DU145, and U87 cells were cultured in RPMI-1640, DMEM and MEM medium, respectively. All media were supplemented with 10% fetal bovine serum (FBS; Valley Biomedical) 2 mmol/L L-glutamine, 100 U/ml penicillin, and 100 μg/ml streptomycin. CAF were cultured in DMEM/F12 supplemented with 5% fetal bovine serum and 5% Nu-serum, 10^{-9} M testosterone 2 mmol/L L-glutamine, 100 U/ml penicillin, and 100 μg/ml streptomycin. Unless otherwise specified, media and supplements were from Invitrogen.

Immunofluorescence microscopy and large oncosome-formation assay

Cell membranes were labeled with FITC-conjugated cholera toxin subunit B (CTxB; Sigma) and analyzed as previously described.[8]

Purification of EV by differential centrifugation

Shed EVs were collected from conditioned media and purified as described.[8] Briefly, 1.6×10^7 cells per plate from 18 150 mm^2 plates, were cultured in serum-free media for 24 h. Culture supernatants was collected and centrifuged at 2800 g for 10 min (4 °C) to eliminate cells and cell debris. Supernatants were sequentially centrifuged (Beckman SW28 rotor) by low g force centrifugation at 10 000 g (30 min, 4 °C), followed by high g force centrifugation at 100 000 g (1 h, 4 °C). After each centrifugation step, EVs were collected from the bottom of the centrifuge tubes using double-filtered (0.22 μm) ice-cold PBS and stored at −80°C.

Patient specimens

Plasma samples used in this study were obtained through an institutional review board approved protocol in compliance with the Declaration of Helsinki. All subjects provided written

informed consent for blood to be used for research purposes. Patient samples were obtained from the Urologic Oncology Program and the Cedars-Sinai BioBank.

EV isolation by filtration

For the isolation of EVs from cultured cells, culture supernatants from 3 150 mm^2 plates or 200 μl of platelet-poor plasma were collected and centrifuged at 2800 g for 10 min to eliminate cells and cell debris. Supernatants were then filtered at 8000 g for 30 s at 4 °C using Vivaspin 500 Ultrafiltration Spin Columns (Sartorius Stedim) with 0.2 μm polyethersulfone (PES) membrane. Large oncosomes, deposited on top of the filter in a volume of 20 μl, and smaller EVs, collected in the filtrate, were recovered and stored at −80 °C.

Immuno-flow cytometry

EVs purified by filtration were fixed in 4% formaldehyde and stained with Cav-1 or ARF6 antibodies (1:200), followed by a FITC- or Cy3-conjugated antibody. EVs were processed on an Aria III Cell Sorter (Becton Dickinson). Background signal was set up on double 0.22 μm filtered PBS, allowing an event rate of 0–4 events/sec using high sheath pressure, whereas sample analyses were performed using low sheath pressure, thus maximizing the amount of scattered light and fluorescence coming from EVs. Light scattering detection was performed in log and linear mode. Bead standards of 1, 2, 4, 6, and 10 μm (Invitrogen) were used to set size gates. At least 3000 events were recorded, and data were analyzed using FlowJo software (Treestar). Comparisons between experimental groups were performed using 2-tailed, unpaired Student *t* test.

Nanoparticle tracking analysis (NTA)

Approximately 300 μl EV suspensions were loaded into the sample chamber of a NanoSight LM20 (NanoSight) using sterile syringes. Videos of 40 or 60 s were recorded for each sample, and particle movement was analyzed by NTA software (version 2.3 Build 0006 BETA2). A minimum of 200 completed particle tracks were analyzed in each video. NTA software settings were: frames per second, 37.80; calibration, 172 nm/pixel; detection threshold, 6–8 Muti; blur, auto; min track length, auto; temperature, 22–25 °C; viscosity, 0.89 cP. Manual shutter and gain adjustments were used during the experiment.[49]

miRNA profiling

Total RNA was extracted from RWPE-1 and RWPE-2 cells as well as from mixed populations of EVs (referred to as EV1 and EV2) purified using the 100 000 g centrifugation, by TRIzol (Invitrogen), and profiled using Affymetrix GeneChip® miRNA Arrays (Affymetrix) containing 847 human mature miRNAs (Asuragen Services). Following incoming sample quality control (QC) assessment, the 3′ ends of RNA molecules in total RNA samples were labeled with biotin according to the company's standard protocol and purified and profiled in duplicate. Hybridization, washing, staining, imaging, and signal extraction were performed according to Affymetrix-recommended procedures. Arrays were scanned on an Affymetrix GeneChip® Scanner 3000 7G. Raw data were normalized by computing the global Variance Stabilization Normalization (VSN)[50] of all the arrays. Each technical duplicate resulted in good signal correlation (**Fig. S1**). Downstream analysis was performed by aggregating single experiment data on a sample basis using the mean. Data were then scaled to assume values above or equal to one. miRNA fold changes and differences were calculated for EV1 over RWPE-1, EV2 over RWPE-2, EV2 over EV1, RWPE-2 over RWPE-1. Fold-change <1 were transformed as $y(x) = (-1/x)$. Due to sample size, no statistical test was applied to assess differential miRNA expression, and data were portrayed as fold change values with a cutoff of 1.5.

Quantitative PCR

For quantitative PCR, total RNA was prepared with the mirVana miRNA isolation kit (Ambion) according to the manufacturer's protocol. Total RNA (15 to 35 ng) was subjected to reverse transcription using the TaqMan MicroRNA Reverse Transcription Kit (Applied Biosystems) with 3 μl of miRNA assay RT primers in a final reaction volume of 15 μl. cDNA was diluted and set up in triplicate qRT-PCRs containing 1 μl of specific TaqMan miRNA assay and run on a ABI 7500 Fast Real-Time PCR System (Applied Biosystem). Data were analyzed by the $\Delta\Delta C_t$ method. Relative expression levels of each miRNA were normalized using EV1, EV2, RWPE-1, and RWPE-2 as reference and RNU6B as endogenous control.[51]

Overexpression of miR-1227

We employed miR-1227 mimic (cat. no. 4464066, specific identifier MC13370), which mimics mature endogenous miRNA, to overexpress miR-1227 in RWPE-2 cells. miRNA mimic negative control (cat. no. 4464058), miR-NC, was used as negative control. Cells were transfected using Lipofectamine™ LTX for the indicated times. The levels of miR-1227 mimic were determined using qRT-PCR and normalized to endogenous control RNU48 expression. All reagents were from Life Technologies.

Proliferation assay and migration assay

Cell proliferation and cell migration of CAF was performed using large EVs from RWPE-2 cells infected with miR-1227 or miR-NC. Both assays were performed as previously described.[52]

miRNA-target gene network and pathway analysis

miRNA targets for miRNAs expressed at significantly differential levels in EV2 than in RWPE-2 cells, but at non-significantly differential levels in EV1 vs. RWPE-1 cells, were identified using Ingenuity Pathway Analysis Software (Ingenuity Systems). miRNA Target Filter was then applied to identify experimentally validated targets in cancer. Selected targets were used to build the miRNA-target gene network and were subjected to systematic network analysis to determine the top biological functions. Right-tailed Fisher exact test ($P < 0.05$) was used to calculate *P* value determining the probability that each biological function assigned to that data set is due to chance alone.

Disclosure of Potential Conflicts of Interest

No potential conflicts of interest were disclosed.

Acknowledgments

The authors thank Dr Beatrice Knudsen for providing access to the Cedars-Sinai BioBank, and Drs Murali Gururajan, Rosalyn M Adam and Samantha Morley for helpful discussions.

Funding

This study was supported by National Cancer Institute (CA131472 [R00] to DDV, R01CA143777 to MRF, the Steven Spielberg Discovery Fund in Prostate Cancer Research to DDV and MRF).

Supplemental Materials

Supplemental materials may be found here: www.landesbioscience.com/journals/cc/article/26539

References

1. Di Vizio D, Morello M, Dudley AC, Schow PW, Adam RM, Morley S, Mulholland D, Rotinen M, Hager MH, Insabato L, et al. Large oncosomes in human prostate cancer tissues and in the circulation of mice with metastatic disease. Am J Pathol 2012; 181:1573-84; PMID:23022210; http://dx.doi.org/10.1016/j.ajpath.2012.07.030
2. Welton JL, Khanna S, Giles PJ, Brennan P, Brewis IA, Staffurth J, Mason MD, Clayton A. Proteomics analysis of bladder cancer exosomes. Mol Cell Proteomics 2010; 9:1324-38; PMID:20224111; http://dx.doi.org/10.1074/mcp.M000063-MCP201
3. Gallo A, Tandon M, Alevizos I, Illei GG. The majority of microRNAs detectable in serum and saliva is concentrated in exosomes. PLoS One 2012; 7:e30679; PMID:22427800; http://dx.doi.org/10.1371/journal.pone.0030679
4. Peinado H, Alečković M, Lavotshkin S, Matei I, Costa-Silva B, Moreno-Bueno G, Hergueta-Redondo M, Williams C, García-Santos G, Ghajar C, et al. Melanoma exosomes educate bone marrow progenitor cells toward a pro-metastatic phenotype through MET. Nat Med 2012; 18:883-91; PMID:22635005; http://dx.doi.org/10.1038/nm.2753
5. Denzer K, Kleijmeer MJ, Heijnen HF, Stoorvogel W, Geuze HJ. Exosome: from internal vesicle of the multivesicular body to intercellular signaling device. J Cell Sci 2000; 113:3365-74; PMID:10984428
6. Silva J, Garcia V, Rodriguez M, Compte M, Cisneros E, Veguillas P, Garcia JM, Dominguez G, Campos-Martin Y, Cuevas J, et al. Analysis of exosome release and its prognostic value in human colorectal cancer. Genes Chromosomes Cancer 2012; 51:409-18; PMID:22420032; http://dx.doi.org/10.1002/gcc.21926
7. Cocucci E, Racchetti G, Meldolesi J. Shedding microvesicles: artefacts no more. Trends Cell Biol 2009; 19:43-51; PMID:19144520; http://dx.doi.org/10.1016/j.tcb.2008.11.003
8. Di Vizio D, Kim J, Hager MH, Morello M, Yang W, Lafargue CJ, True LD, Rubin MA, Adam RM, Beroukhim R, et al. Oncosome formation in prostate cancer: association with a region of frequent chromosomal deletion in metastatic disease. Cancer Res 2009; 69:5601-9; PMID:19549916; http://dx.doi.org/10.1158/0008-5472.CAN-08-3860
9. Hager MH, Morley S, Bielenberg DR, Gao S, Morello M, Holcomb IN, Liu W, Mouneimne G, Demichelis F, Kim J, et al. DIAPH3 governs the cellular transition to the amoeboid tumour phenotype. EMBO Mol Med 2012; 4:743-60; PMID:22593025; http://dx.doi.org/10.1002/emmm.201200242
10. Valadi H, Ekström K, Bossios A, Sjöstrand M, Lee JJ, Lötvall JO. Exosome-mediated transfer of mRNAs and microRNAs is a novel mechanism of genetic exchange between cells. Nat Cell Biol 2007; 9:654-9; PMID:17486113; http://dx.doi.org/10.1038/ncb1596
11. Bellingham SA, Coleman BM, Hill AF. Small RNA deep sequencing reveals a distinct miRNA signature released in exosomes from prion-infected neuronal cells. Nucleic Acids Res 2012; 40:10937-49; PMID:22965126; http://dx.doi.org/10.1093/nar/gks832
12. Muralidharan-Chari V, Clancy J, Plou C, Romao M, Chavrier P, Raposo G, D'Souza-Schorey C. ARF6-regulated shedding of tumor cell-derived plasma membrane microvesicles. Curr Biol 2009; 19:1875-85; PMID:19896381; http://dx.doi.org/10.1016/j.cub.2009.09.059
13. Wright M. Nanoparticle tracking analysis for the multiparameter characterization and counting of nanoparticle suspensions. Methods Mol Biol 2012; 906:511-24; PMID:22791460
14. Chen WW, Balaj L, Liau LM, Samuels ML, Kotsopoulos SK, Maguire CA, Loguidice L, Soto H, Garrett M, Zhu LD, et al. BEAMing and Droplet Digital PCR Analysis of Mutant IDH1 mRNA in Glioma Patient Serum and Cerebrospinal Fluid Extracellular Vesicles. Mol Ther Nucleic Acids 2013; 2:e109; PMID:23881452; http://dx.doi.org/10.1038/mtna.2013.28
15. Bello D, Webber MM, Kleinman HK, Wartinger DD, Rhim JS. Androgen responsive adult human prostatic epithelial cell lines immortalized by human papillomavirus 18. Carcinogenesis 1997; 18:1215-23; PMID:9214605; http://dx.doi.org/10.1093/carcin/18.6.1215
16. Lian J, Zhang X, Tian H, Liang N, Wang Y, Liang C, Li X, Sun F. Altered microRNA expression in patients with non-obstructive azoospermia. Reprod Biol Endocrinol 2009; 7:13; PMID:19210773; http://dx.doi.org/10.1186/1477-7827-7-13
17. Liu C, Cheng H, Shi S, Cui X, Yang J, Chen L, Cen P, Cai X, Lu Y, Wu C, et al. MicroRNA-34b inhibits pancreatic cancer metastasis through repressing Smad3. Curr Mol Med 2013; 13:467-78; PMID:23305226; http://dx.doi.org/10.2174/1566524011313040001
18. Katayama Y, Maeda M, Miyaguchi K, Nemoto S, Yasen M, Tanaka S, Mizushima H, Fukuoka Y, Arii S, Tanaka H. Identification of pathogenesis-related microRNAs in hepatocellular carcinoma by expression profiling. Oncol Lett 2012; 4:817-23; PMID:23205106
19. Yang B, Jing C, Wang J, Guo X, Chen Y, Xu R, Peng L, Liu J, Li L. Identification of microRNAs associated with lymphangiogenesis in human gastric cancer. Clin Transl Oncol 2013; PMID:23881463; http://dx.doi.org/10.1007/s12094-013-1081-6
20. Salim H, Akbar NS, Zong D, Vaculova AH, Lewensohn R, Moshfegh A, Viktorsson K, Zhivotovsky B. miRNA-214 modulates radiotherapy response of non-small cell lung cancer cells through regulation of p38MAPK, apoptosis and senescence. Br J Cancer 2012; 107:1361-73; PMID:22929890; http://dx.doi.org/10.1038/bjc.2012.382
21. Mitchell PS, Parkin RK, Kroh EM, Fritz BR, Wyman SK, Pogosova-Agadjanyan EL, Peterson A, Noteboom J, O'Briant KC, Allen A, et al. Circulating microRNAs as stable blood-based markers for cancer detection. Proc Natl Acad Sci U S A 2008; 105:10513-8; PMID:18663219; http://dx.doi.org/10.1073/pnas.0804549105
22. Bryant RJ, Pawlowski T, Catto JW, Marsden G, Vessella RL, Rhees B, Kuslich C, Visakorpi T, Hamdy FC. Changes in circulating microRNA levels associated with prostate cancer. Br J Cancer 2012; 106:768-74; PMID:22240788; http://dx.doi.org/10.1038/bjc.2011.595
23. Wang N, Li Q, Feng NH, Cheng G, Guan ZL, Wang Y, Qin C, Yin CJ, Hua LX. miR-205 is frequently downregulated in prostate cancer and acts as a tumor suppressor by inhibiting tumor growth. Asian J Androl 2013; PMID:23974361; http://dx.doi.org/10.1038/aja.2013.80
24. Dakhova O, Ozen M, Creighton CJ, Li R, Ayala G, Rowley D, Ittmann M. Global gene expression analysis of reactive stroma in prostate cancer. Clin Cancer Res 2009; 15:3979-89; PMID:19509179; http://dx.doi.org/10.1158/1078-0432.CCR-08-1899
25. Tahir SA, Yang G, Ebara S, Timme TL, Satoh T, Li L, Goltsov A, Ittmann M, Morrisett JD, Thompson TC. Secreted caveolin-1 stimulates cell survival/clonal growth and contributes to metastasis in androgen-insensitive prostate cancer. Cancer Res 2001; 61:3882-5; PMID:11358800
26. Tauro BJ, Greening DW, Mathias RA, Ji H, Mathivanan S, Scott AM, Simpson RJ. Comparison of ultracentrifugation, density gradient separation, and immunoaffinity capture methods for isolating human colon cancer cell line LIM1863-derived exosomes. Methods 2012; 56:293-304; PMID:22285593; http://dx.doi.org/10.1016/j.ymeth.2012.01.002
27. Lee TH, D'Asti E, Magnus N, Al-Nedawi K, Meehan B, Rak J. Microvesicles as mediators of intercellular communication in cancer--the emerging science of cellular 'debris'. Semin Immunopathol 2011; 33:455-67; PMID:21318413; http://dx.doi.org/10.1007/s00281-011-0250-3
28. D'Souza-Schorey C, Clancy JW. Tumor-derived microvesicles: shedding light on novel microenvironment modulators and prospective cancer biomarkers. Genes Dev 2012; 26:1287-99; PMID:22713869; http://dx.doi.org/10.1101/gad.192351.112
29. D'Asti E, Garnier D, Lee TH, Montermini L, Meehan B, Rak J. Oncogenic extracellular vesicles in brain tumor progression. Front Physiol 2012; 3:294; PMID:22934045
30. Torres A, Torres K, Pesci A, Ceccaroni M, Paszkowski T, Cassandrini P, Zamboni G, Maciejewski R. Diagnostic and prognostic significance of miRNA signatures in tissues and plasma of endometrioid endometrial carcinoma patients. Int J Cancer 2013; 132:1633-45; PMID:22987275; http://dx.doi.org/10.1002/ijc.27840
31. Jaiswal R, Luk F, Gong J, Mathys JM, Grau GE, Bebawy M. Microparticle conferred microRNA profiles--implications in the transfer and dominance of cancer traits. Mol Cancer 2012; 11:37; PMID:22682234; http://dx.doi.org/10.1186/1476-4598-11-37
32. Collino F, Deregibus MC, Bruno S, Sterpone L, Aghemo G, Viltono L, Tetta C, Camussi G. Microvesicles derived from adult human bone marrow and tissue specific mesenchymal stem cells shuttle selected pattern of miRNAs. PLoS One 2010; 5:e11803; PMID:20668554; http://dx.doi.org/10.1371/journal.pone.0011803
33. Palma J, Yaddanapudi SC, Pigati L, Havens MA, Jeong S, Weiner GA, Weimer KM, Stern B, Hastings ML, Duelli DM. MicroRNAs are exported from malignant cells in customized particles. Nucleic Acids Res 2012; 40:9125-38; PMID:22772984; http://dx.doi.org/10.1093/nar/gks656

34. Taylor DD, Gercel-Taylor C. MicroRNA signatures of tumor-derived exosomes as diagnostic biomarkers of ovarian cancer. Gynecol Oncol 2008; 110:13-21; PMID:18589210; http://dx.doi.org/10.1016/j.ygyno.2008.04.033
35. Nicoloso MS, Spizzo R, Shimizu M, Rossi S, Calin GA. MicroRNAs--the micro steering wheel of tumour metastases. Nat Rev Cancer 2009; 9:293-302; PMID:19262572; http://dx.doi.org/10.1038/nrc2619
36. Chen ML, Liang LS, Wang XK. miR-200c inhibits invasion and migration in human colon cancer cells SW480/620 by targeting ZEB1. Clin Exp Metastasis 2012; 29:457-69; PMID:22407310; http://dx.doi.org/10.1007/s10585-012-9463-7
37. Puhr M, Hoefer J, Schäfer G, Erb HH, Oh SJ, Klocker H, Heidegger I, Neuwirt H, Culig Z. Epithelial-to-mesenchymal transition leads to docetaxel resistance in prostate cancer and is mediated by reduced expression of miR-200c and miR-205. Am J Pathol 2012; 181:2188-201; PMID:23041061; http://dx.doi.org/10.1016/j.ajpath.2012.08.011
38. Yang WH, Lan HY, Huang CH, Tai SK, Tzeng CH, Kao SY, Wu KJ, Hung MC, Yang MH. RAC1 activation mediates Twist1-induced cancer cell migration. Nat Cell Biol 2012; 14:366-74; PMID:22407364; http://dx.doi.org/10.1038/ncb2455
39. Majid S, Dar AA, Saini S, Arora S, Shahryari V, Zaman MS, Chang I, Yamamura S, Tanaka Y, Deng G, et al. miR-23b represses proto-oncogene Src kinase and functions as methylation-silenced tumor suppressor with diagnostic and prognostic significance in prostate cancer. Cancer Res 2012; 72:6435-46; PMID:23074286; http://dx.doi.org/10.1158/0008-5472.CAN-12-2181
40. Tong AW, Fulgham P, Jay C, Chen P, Khalil I, Liu S, Senzer N, Eklund AC, Han J, Nemunaitis J. MicroRNA profile analysis of human prostate cancers. Cancer Gene Ther 2009; 16:206-16; PMID:18949015
41. Polytarchou C, Iliopoulos D, Struhl K. An integrated transcriptional regulatory circuit that reinforces the breast cancer stem cell state. Proc Natl Acad Sci U S A 2012; 109:14470-5; PMID:22908280; http://dx.doi.org/10.1073/pnas.1212811109
42. Hu H, Li S, Liu J, Ni B. MicroRNA-193b modulates proliferation, migration, and invasion of non-small cell lung cancer cells. Acta Biochim Biophys Sin (Shanghai) 2012; 44:424-30; PMID:22491710; http://dx.doi.org/10.1093/abbs/gms018
43. Xu C, Liu S, Fu H, Li S, Tie Y, Zhu J, Xing R, Jin Y, Sun Z, Zheng X. MicroRNA-193b regulates proliferation, migration and invasion in human hepatocellular carcinoma cells. Eur J Cancer 2010; 46:2828-36; PMID:20655737; http://dx.doi.org/10.1016/j.ejca.2010.06.127
44. Boll K, Reiche K, Kasack K, Mörbt N, Kretzschmar AK, Tomm JM, Verhaegh G, Schalken J, von Bergen M, Horn F, et al. MiR-130a, miR-203 and miR-205 jointly repress key oncogenic pathways and are downregulated in prostate carcinoma. Oncogene 2013; 32:277-85; PMID:22391564
45. Au SL, Wong CC, Lee JM, Fan DN, Tsang FH, Ng IO, Wong CM. Enhancer of zeste homolog 2 epigenetically silences multiple tumor suppressor microRNAs to promote liver cancer metastasis. Hepatology 2012; 56:622-31; PMID:22370893; http://dx.doi.org/10.1002/hep.25679
46. Gandellini P, Profumo V, Casamichele A, Fenderico N, Borrelli S, Petrovich G, Santilli G, Callari M, Colecchia M, Pozzi S, et al. miR-205 regulates basement membrane deposition in human prostate: implications for cancer development. Cell Death Differ 2012; 19:1750-60; PMID:22555458; http://dx.doi.org/10.1038/cdd.2012.56
47. Gandellini B, Folini M, Longoni N, Pennati M, Binda M, Colecchia M, Salvioni R, Supino R, Moretti R, Limonta P, et al. miR-205 Exerts tumor-suppressive functions in human prostate through down-regulation of protein kinase Cepsilon. Cancer Res 2009; 69:2287-95; PMID:19244118; http://dx.doi.org/10.1158/0008-5472.CAN-08-2894
48. Gandellini P, Giannoni E, Casamichele A, Taddei ML, Callari M, Piovan C, Valdagni R, Pierotti MA, Zaffaroni N, Chiarugi P. miR-205 hinders the malignant interplay between prostate cancer cells and associated fibroblasts. Antioxid Redox Signal 2013; PMID:23924028; http://dx.doi.org/10.1089/ars.2013.5292
49. Dragovic RA, Gardiner C, Brooks AS, Tannetta DS, Ferguson DJ, Hole P, Carr B, Redman CW, Harris AL, Dobson PJ, et al. Sizing and phenotyping of cellular vesicles using Nanoparticle Tracking Analysis. Nanomedicine 2011; 7:780-8; PMID:21601655; http://dx.doi.org/10.1016/j.nano.2011.04.003
50. Huber W, von Heydebreck A, Sültmann H, Poustka A, Vingron M. Variance stabilization applied to microarray data calibration and to the quantification of differential expression. Bioinformatics 2002; 18(Suppl 1):S96-104; PMID:12169536; http://dx.doi.org/10.1093/bioinformatics/18.suppl_1.S96
51. Gordanpour A, Nam RK, Sugar L, Bacopulos S, Seth A. MicroRNA detection in prostate tumors by quantitative real-time PCR (qPCR). J Vis Exp 2012; e3874; PMID:22643910
52. Ayala G, Morello M, Frolov A, You S, Li R, Rosati F, Bartolucci G, Danza G, Adam RM, Thompson TC, et al. Loss of caveolin-1 in prostate cancer stroma correlates with reduced relapse-free survival and is functionally relevant to tumour progression. J Pathol 2013; 231:77-87; PMID:23729330; http://dx.doi.org/10.1002/path.4217